

Evaluating the boundary and Stieltjes transform of limiting spectral distributions for random matrices with a separable variance profile

William Leeb*

Abstract

We present numerical algorithms for solving two problems encountered in random matrix theory and its applications. First, we compute the boundary of the limiting spectral distribution for random matrices with a separable variance profile. Second, we evaluate the Stieltjes transform of such a distribution at real values exceeding the boundary. Both problems are solved with the use of Newton's method. We prove the correctness of the algorithms from a detailed analysis of the master equations that characterize the Stieltjes transform. We demonstrate the algorithms' performance in several experiments.

1 Introduction

This paper presents fast, scalable, and numerically stable algorithms for the solution of two related problems that arise in high-dimensional statistics. To describe these two problems, we suppose we have a k -by- l random matrix of the form $\mathbf{N} = \mathbf{A}^{1/2} \mathbf{G} \mathbf{B}^{1/2}$, where \mathbf{G} is a random matrix with iid entries of mean zero and variance l^{-1} , and \mathbf{A} and \mathbf{B} are positive-definite matrices of sizes k -by- k and l -by- l , respectively. We are interested in certain limiting behaviors of the *empirical spectral distribution (ESD)* μ_k , which is the distribution of eigenvalues $\lambda_1, \dots, \lambda_k$ of the matrix of $\mathbf{N} \mathbf{N}^T$:

$$d\mu_k(t) = \frac{1}{k} \sum_{i=1}^k \delta_{\lambda_i}(t). \quad (1)$$

Under suitable conditions on \mathbf{A} and \mathbf{B} , as k and $l = l_k$ both grow to infinity so that the ratio $k/l \rightarrow \gamma > 0$, the sequence of measures μ_k will almost surely converge weakly to a compactly supported measure μ , called the *limiting spectral distribution (LSD)*.

With this background, we may now state our results. First, we will present an algorithm to determine the right endpoint of the LSD's support. That is, we compute:

$$\lambda^* = \arg \max\{\lambda > 0 : \mu([\lambda, \infty)) > 0\}. \quad (2)$$

Second, we will present an algorithm to evaluate the *Stieltjes transform* $s(\lambda)$ of μ , and its derivative, at values $\lambda > \lambda^*$. That is, we will evaluate the integrals

$$s(\lambda) = \int_{\mathbb{R}} \frac{1}{t - \lambda} d\mu(t), \quad (3)$$

and

$$s'(\lambda) = \int_{\mathbb{R}} \frac{1}{(t - \lambda)^2} d\mu(t), \quad (4)$$

at any value $\lambda > \lambda^*$.

Our primary motivation for studying these problems is their application to matrix denoising and principal component analysis in high dimensions. Specifically, in signal-plus-noise matrix models of the kind studied in [2, 27, 10, 25, 13, 30, 24, 12, 18, 16, 35, 17], the relationship between the singular value decompositions of the signal matrix and the observed matrix can be quantified by the Stieltjes transform of the LSD of the noise matrix, evaluated at positive numbers outside the LSD's support. Furthermore, identifying the boundary of the LSD is useful for separating the noise and signal components in such a model. Estimating the number of signal terms in principal components analysis and factor models is a well-studied problem in statistics [11, 9, 3, 19, 20, 29, 21]. We note too that random matrices with separable variance profiles arise naturally in wireless communications [5] and have been subject to extensive theoretical analysis [6, 15, 14].

The solution to both problems we study rests on a well-known characterization of the Stieltjes transform of μ as the solution to a certain non-linear equation [31, 6]. We present a detailed analysis of this equation, and prove that both the problems of finding the bulk edge and evaluating the Stieltjes transform may be solved by Newton's root-finding algorithm, appropriately initialized and implemented.

*School of Mathematics, University of Minnesota, Twin Cities. Minneapolis, MN, USA.

In order to have a well-defined LSD, we assume that the spectra of \mathbf{A} and \mathbf{B} have limiting distributions ν and $\underline{\nu}$, respectively. In this paper, we consider the setting where ν and $\underline{\nu}$ are discrete distributions of the form

$$d\nu = \sum_{i=1}^p \omega_i \delta_{a_i} \quad (5)$$

and

$$d\underline{\nu} = \sum_{j=1}^n \pi_j \delta_{b_j}. \quad (6)$$

Here, a_1, \dots, a_p and b_1, \dots, b_n are positive numbers, and the weights ω_i and π_j satisfy $\sum_{i=1}^p \omega_i = \sum_{j=1}^n \pi_j = 1$, $\omega_i > 0$, and $\pi_j > 0$. For example, if $k/2$ eigenvalues of \mathbf{A} are 1, and the remaining $k/2$ are equal to 2, then $p = 2$, $a_1 = 1$, $a_2 = 2$, and $\omega_1 = \omega_2 = 2$.

Previous works have considered the problem of evaluating the LSD, its Stieltjes transform, and the boundary of its support, for singly-weighted random matrices (where $\mathbf{B} = \mathbf{I}_l$). The paper [8] proposes a scheme for evaluating the Stieltjes transform at complex values outside the support of the LSD; this method is based on a non-linear equation satisfied by the Stieltjes transform [32, 33, 26]. The method in [4] is devoted to extending the approach to mixture models. The papers [22, 23] are concerned with solving the inverse problem of recovering the population distribution from the observed spectrum. The paper [11] contains a method for finding the boundary of the LSD based on root-finding, although the use of Newton's method is not employed or analyzed.

The algorithms we present here are applicable for general \mathbf{A} and \mathbf{B} , and are provably fast and numerically accurate. The speed and accuracy are consequences of the use of Newton's method, which exhibits quadratic convergence. Indeed, the primary mathematical content of this paper is to show that for both problems considered, Newton's method may be applied. Consequently, all parameters we compute are either available analytically, or can be computed by a rapidly converging iterative scheme.

The remainder of the paper is outlined as follows. In Section 2, we review the mathematical and numerical material that we will be using. In Section 3, we derive the core mathematical theory on which our algorithms rest, namely a detailed analysis of the master equations characterizing the Stieltjes transform of μ . In Section 4, we provide explicit descriptions of the numerical algorithms for finding the boundary and evaluating the Stieltjes transform. In Section 5, we present the results of several illustrative numerical experiments demonstrating the performance of our algorithms.

2 Preliminaries

In this section, we will review known results from random matrix theory and optimization that we will make use of throughout this paper. Throughout the exposition, we suppose we have a random matrix \mathbf{G} of size k -by- l , with iid entries of mean zero and variance l^{-1} . For simplicity, the reader may assume the entries are Gaussian, though this assumption can be relaxed. We consider the matrix $\mathbf{N} = \mathbf{A}^{1/2} \mathbf{G} \mathbf{B}^{1/2}$, where \mathbf{A} and \mathbf{B} are positive-definite matrices. We suppose that $l = l_k$ grows with k , and that the limit

$$\gamma = \lim_{k \rightarrow \infty} \frac{k}{l_k} \quad (7)$$

is well-defined, positive, and finite. Furthermore, as k and l grow, we suppose that the spectra of \mathbf{A} and \mathbf{B} have well-defined asymptotic distributions ν and $\underline{\nu}$, respectively (in terms of weak convergence). We denote by μ the limiting spectral distribution of the eigenvalues of $\mathbf{N} \mathbf{N}^T$, and by $\underline{\mu}$ the limiting spectral distribution of the eigenvalues of $\mathbf{N}^T \mathbf{N}$.

2.1 The Stieltjes transform of the LSD

The Stieltjes transform of the LSD μ is defined for λ outside μ 's support by:

$$s(\lambda) = \int_{\mathbb{R}} \frac{1}{t - \lambda} d\mu(t). \quad (8)$$

The Stieltjes transform of the spectral distribution $\underline{\mu}$ of $\mathbf{N}^T \mathbf{N}$ is similarly defined by

$$\underline{s}(\lambda) = \int_{\mathbb{R}} \frac{1}{t - \lambda} d\underline{\mu}(t). \quad (9)$$

We call $\underline{s}(\lambda)$ the *associated Stieltjes transform* of μ . We refer the reader to the standard references [1, 34] for a detailed treatment.

It is easy to see that μ and $\underline{\mu}$ are related by the following formulas:

$$d\underline{\mu}(t) = \gamma d\mu(t) + (1 - \gamma) \delta_0(t) \quad (10)$$

and inverting this:

$$d\mu(t) = \frac{1}{\gamma} d\underline{\mu}(t) + \left(1 - \frac{1}{\gamma}\right) \delta_0(t). \quad (11)$$

Consequently, we have the following relations between the Stieltjes transforms $s(\lambda)$ and $\underline{s}(\lambda)$:

$$\underline{s}(\lambda) = \gamma s(\lambda) + \frac{\gamma - 1}{\lambda} \quad (12)$$

and

$$s(\lambda) = \frac{1}{\gamma} \underline{s}(\lambda) + \left(\frac{1}{\gamma} - 1\right) \frac{1}{\lambda}. \quad (13)$$

We also have the following relations between their derivatives, $s'(\lambda)$ and $\underline{s}'(\lambda)$:

$$\underline{s}'(\lambda) = \gamma s'(\lambda) + \frac{1 - \gamma}{\lambda^2} \quad (14)$$

and

$$s'(\lambda) = \frac{1}{\gamma} \underline{s}'(\lambda) + \left(1 - \frac{1}{\gamma}\right) \frac{1}{\lambda^2}. \quad (15)$$

2.2 The master equations for $s(\lambda)$

It has been shown that the Stieltjes transform $s(\lambda)$ for the LSD satisfies the following *master equations*:

$$s(\lambda) = \int_{\mathbb{R}} \frac{1}{aG(e(\lambda)) - \lambda} d\nu(a), \quad (16)$$

where

$$G(e) = \int_{\mathbb{R}} \frac{b}{1 + \gamma b e} d\underline{\nu}(b) \quad (17)$$

and $e(\lambda)$ is a function that satisfies the equation

$$e(\lambda) = \int_{\mathbb{R}} \frac{a}{aG(e(\lambda)) - \lambda} d\nu(a). \quad (18)$$

See, for instance, the paper [31]. The paper [6] presents a slightly modified form of these equations, with a detailed analysis showing that $e(\lambda)$ is smooth for real λ outside the support of μ .

We assume that ν and $\underline{\nu}$ are discrete measures of the form

$$d\nu = \sum_{i=1}^p \omega_i \delta_{a_i}, \quad (19)$$

and

$$d\underline{\nu} = \sum_{j=1}^n \pi_j \delta_{b_j}, \quad (20)$$

where $\sum_{i=1}^p \omega_i = \sum_{j=1}^n \pi_j = 1$, $\omega_i > 0$, and $\pi_j > 0$. The master equations therefore become:

$$s(\lambda) = \sum_{i=1}^p \frac{\omega_i}{a_i G(e(\lambda)) - \lambda} \quad (21)$$

where $e(\lambda)$ is a function satisfying

$$e(\lambda) = \sum_{i=1}^p \frac{a_i \omega_i}{a_i G(e(\lambda)) - \lambda} \quad (22)$$

and the function G is defined by:

$$G(e) = \sum_{j=1}^n \frac{b_j \pi_j}{1 + \gamma b_j e}. \quad (23)$$

We note that in the case where $\mathbf{B} = \mathbf{I}_n$ (the singly-weighted case), the master equations take on a simpler form; see, for instance, [33, 32].

2.3 The D -transform and the spiked model

In a spiked matrix model, we observe a signal-plus-noise matrix \mathbf{Y} of the form

$$\mathbf{Y} = \mathbf{X} + \mathbf{N}, \quad (24)$$

where $\mathbf{X} = \sum_{m=1}^r \theta_m \mathbf{u}_m \mathbf{v}_m^T$ is a rank $r \ll \min\{k, l\}$ signal matrix, and \mathbf{N} is a noise matrix. The D -transform, introduced in [2], is defined as follows:

$$D(\sigma) = \sigma^2 s(\sigma^2) \underline{s}(\sigma^2), \quad (25)$$

where $s(\lambda)$ and $\underline{s}(\lambda)$ are, respectively, the Stieltjes transform and associated Stieltjes transform of the LSD of $\mathbf{N}\mathbf{N}^T$.

Denoting by $\sigma_1, \dots, \sigma_r$ the top r singular values of \mathbf{Y} , and $\hat{\mathbf{u}}_1, \dots, \hat{\mathbf{u}}_r, \hat{\mathbf{v}}_1, \dots, \hat{\mathbf{v}}_r$ the corresponding left and right singular vectors, respectively, it is shown in [2] that the D -transform defines a mapping between $\sigma_1, \dots, \sigma_r$ and the singular values $\theta_1, \dots, \theta_r$ of the signal matrix \mathbf{X} , which holds in the limit $k \rightarrow \infty$:

$$\theta_m = \sqrt{\frac{1}{D(\sigma_m)}}. \quad (26)$$

This is satisfied for sufficiently large singular values θ_m of \mathbf{X} , namely those for which $\theta_m > D(\sqrt{\lambda^*})^{-1/2}$.

Furthermore, the asymptotic cosines $\langle \mathbf{u}_m, \hat{\mathbf{u}}_m \rangle$ and $\langle \mathbf{v}_m, \hat{\mathbf{v}}_m \rangle$, $1 \leq m \leq r$, can also be evaluated using the Stieltjes transform. It is shown that

$$\lim_{k \rightarrow \infty} |\langle \mathbf{u}_m, \hat{\mathbf{u}}_m \rangle|^2 = \frac{-2\sigma_m s(\sigma_m^2)}{\theta_m^2 D'(\sigma_m)}, \quad (27)$$

and

$$\lim_{k \rightarrow \infty} |\langle \mathbf{v}_m, \hat{\mathbf{v}}_m \rangle|^2 = \frac{-2\sigma_m \underline{s}(\sigma_m^2)}{\theta_m^2 D'(\sigma_m)}. \quad (28)$$

Consequently, evaluating $s(\sigma_m^2)$ and $s'(\sigma_m^2)$ provides a method for estimating the angles between the population singular vectors $\mathbf{u}_m, \mathbf{v}_m$ and the observed singular vectors $\hat{\mathbf{u}}_m, \hat{\mathbf{v}}_m$. These relationships have been employed to derive optimal methods of singular value shrinkage [27].

2.4 Newton's root-finding algorithm

Newton's method is a classical technique for finding the roots of a function of one real variable. We briefly review the method here; the reader may consult any standard reference on optimization or numerical analysis, such as [28, 7], for additional details. We are given a smooth function $f(x)$, where $x \in [a, b]$, and we suppose $f(a) < 0$ and $f(b) > 0$. We also suppose that $f'(x) > 0$ and $f''(x) < 0$ for all $x \in (a, b)$; that is, f is a strictly increasing and concave. Our goal is to compute x^* , the unique root of f in (a, b) .

To find x^* , Newton's method initializes $a < x_0 < x^*$, and defines a sequence of updates recursively as follows: given an estimate x_k , the next value x_{k+1} is defined by

$$x_{k+1} = x_k - \frac{f(x_k)}{f'(x_k)}. \quad (29)$$

Geometrically, x_{k+1} is the root of the line tangent to the graph of f at the point $(x_k, f(x_k))$. Because f is concave, it is easy to see that $x_k < x_{k+1} \leq x^*$.

Because each x_k is obtained from a linear approximation to f , the errors decay quadratically in the vicinity of x^* ; that is

$$|x_{k+1} - x^*| \leq C|x_k - x^*|^2 \quad (30)$$

when $|x_k - x^*|$ is sufficiently small. The quadratic convergence is what makes Newton's method an especially attractive algorithm when it is applicable. In practical terms, it means that the number of accurately computed digits of x^* approximately doubles on each iteration of the algorithm, until machine precision is reached.

3 Mathematical apparatus

In this section, we analyze the master equations (21) – (23). Our results will provide the necessary tools to devise algorithms for computing the right boundary of μ and evaluating $s(\lambda)$ and $s'(\lambda)$ to the right of the boundary. Throughout, we will denote by λ^* the right edge of the support of μ . We let $a^* = \max_{1 \leq i \leq p} a_i$, and $b^* = \max_{1 \leq j \leq n} b_j$.

We define the function $F(\lambda, e)$ by:

$$F(\lambda, e) = e - \sum_{i=1}^p \frac{a_i \omega_i}{a_i G(e) - \lambda}. \quad (31)$$

Then for each $\lambda > \lambda^*$, $e(\lambda)$ satisfies $F(\lambda, e(\lambda)) = 0$. When we treat λ as a fixed parameter and e as a variable, we will use the notation $F_\lambda(e) = F(\lambda, e)$.

3.1 Range and monotonicity of $e(\lambda)$ when $\lambda > \lambda^*$

We first state a result on the range of $e(\lambda)$ for $\lambda > \lambda^*$. The function $G(e)$ approaches 0 as $e \rightarrow \infty$, and grows to $+\infty$ as $e \rightarrow (-1/\gamma b^*)^+$, and is strictly decreasing on the interval

$$J \equiv \left\{ e : e > \frac{-1}{\gamma b^*} \right\}. \quad (32)$$

For any $\lambda > 0$, we define the interval I_λ by

$$I_\lambda \equiv \left\{ e \in J : G(e) < \frac{\lambda}{a^*} \right\}. \quad (33)$$

Proposition 3.1. *When $\lambda > \lambda^*$, $e(\lambda)$ is contained in the interval $I_\lambda \cap (-\infty, 0)$.*

We will develop the proof in several steps.

Lemma 3.2. *Let $\epsilon > 0$. Then the function $G(e(\lambda))$ is bounded for all $\lambda > \lambda^* + \epsilon$.*

Proof. We show that the range of $e(\lambda)$ cannot approach any of the singularities of G , which lie at the values $-1/(\gamma b_j)$. Define

$$H(\lambda) = \frac{G(e(\lambda))}{\lambda}. \quad (34)$$

Then from (21)

$$\lambda s(\lambda) = \sum_{i=1}^p \frac{\omega_i}{a_i H(\lambda) - 1}, \quad (35)$$

and consequently

$$1 + \lambda s(\lambda) = \sum_{i=1}^p \frac{\omega_i}{a_i H(\lambda) - 1} + \sum_{i=1}^p \omega_i \frac{a_i H(\lambda) - 1}{a_i H(\lambda) - 1} = \sum_{i=1}^p \frac{a_i H(\lambda) \omega_i}{a_i H(\lambda) - 1} = G(e(\lambda)) e(\lambda). \quad (36)$$

Since $\lambda s(\lambda)$ is bounded for $\lambda > \lambda^* + \epsilon$, this tells us that $G(e(\lambda))$ must stay bounded so long as $e(\lambda)$ is bounded away from 0; in particular, $e(\lambda)$ cannot be made arbitrarily close to any of the singularities $-1/(\gamma b_j)$. \square

Corollary 3.3. *$e(\lambda) \rightarrow 0^-$ as $\lambda \rightarrow \infty$.*

Proof. Because $G(e(\lambda))$ is bounded for large λ , the result follows from (22). \square

Corollary 3.4. *For any $\lambda > \lambda^*$, $e(\lambda) \in J$; that is,*

$$e(\lambda) > \frac{-1}{\gamma b^*}. \quad (37)$$

Proof. This follows from the continuity of $e(\lambda)$ for $\lambda > \lambda^*$, and the facts that it never passes through $-1/(\gamma b_j)$ and approaches 0 at large λ . \square

Corollary 3.5. *For all $\lambda > \lambda^*$, $G(e(\lambda)) > 0$ and $e(\lambda) < 0$.*

Proof. The positivity of $G(e(\lambda))$ follows immediately from Corollary 3.4. The negativity of $e(\lambda)$ then follows from (36), and the fact that $1 + \lambda s(\lambda) < 0$. \square

Lemma 3.6. *For all $\lambda > \lambda^*$,*

$$\frac{G(e(\lambda))}{\lambda} < \frac{1}{a^*}. \quad (38)$$

Proof. We have $G(e(\lambda)) \neq \lambda/a_i$, from (21). Suppose for some $\lambda > \lambda^*$, we had

$$\frac{G(e(\lambda))}{\lambda} > \frac{1}{a_i}. \quad (39)$$

The inequality must then remain true for all sufficiently large λ , since $G(e(\lambda))/\lambda$ is continuous and does not pass through $1/a_i$. However, the left side converges to 0 as $\lambda \rightarrow \infty$, since $G(e(\lambda))$ is bounded for large λ ; a contradiction. This completes the proof. \square

We have shown that for all $\lambda > \lambda^*$, $e(\lambda)$ lies in the interval defined by the inequalities

$$G(e) \leq \frac{\lambda}{a^*}, \quad e > \frac{-1}{\gamma b^*}, \quad e < 0. \quad (40)$$

This completes the proof of Proposition 3.1.

Next we prove that $e(\lambda)$ is increasing:

Proposition 3.7. *The function $e(\lambda)$ is increasing for $\lambda > \lambda^*$.*

Proof. We have:

$$(\partial_\lambda F)(\lambda, e) = - \sum_{i=1}^p \frac{a_i \omega_i}{(a_i G(e) - \lambda)^2} < 0. \quad (41)$$

Since $F(\lambda, e(\lambda)) = 0$, we have:

$$0 = \frac{\partial}{\partial \lambda} \{F(\lambda, e(\lambda))\} = (\partial_\lambda F)(\lambda, e(\lambda)) + e'(\lambda)(\partial_e F)(\lambda, e(\lambda)), \quad (42)$$

and so

$$e'(\lambda)(\partial_e F)(\lambda, e(\lambda)) = \sum_{i=1}^p \frac{a_i \omega_i}{(a_i G(e) - \lambda)^2} > 0. \quad (43)$$

Consequently, $e'(\lambda)$ can never be 0. Furthermore,

$$(\partial_e F)(\lambda, e) = 1 + G'(e(\lambda)) \sum_{i=1}^p \left(\frac{a_i}{a_i G(e(\lambda)) - \lambda} \right)^2 \omega_i \quad (44)$$

which converges to 1 as $\lambda \rightarrow \infty$ (note that $e(\lambda)$ stays bounded away from singularities of $G(e)$ and also $G'(e)$, which have the same singularities). So $e'(\lambda) > 0$ for sufficiently large λ , and hence, since it is continuous and cannot pass through 0, $e'(\lambda) > 0$ for all $\lambda > \lambda^*$. \square

3.2 Behavior of $F_\lambda(e)$

In this section we characterize the behavior of $F_\lambda(e) = F(\lambda, e)$ (viewed as a function of e) on the interval I_λ . Specifically, we show the following. For any $\lambda > 0$, $F_\lambda(e)$ is a strictly convex function that approaches $+\infty$ as e approaches either end of I_λ . Furthermore, when $\lambda > \lambda^*$, the minimum value of $F_\lambda(e)$ is less than zero, and $F_\lambda(0) > 0$; consequently, there are exactly two roots of $F_\lambda(e)$, both contained in the interval $I_\lambda \cap (-\infty, 0)$. We show that $e(\lambda)$ is always equal to the largest root, namely the one at which $F'_\lambda(e) > 0$.

In Figure 1, we plot the function $F_\lambda(e)$ on the domain I_λ for a value $\lambda > \lambda^*$.

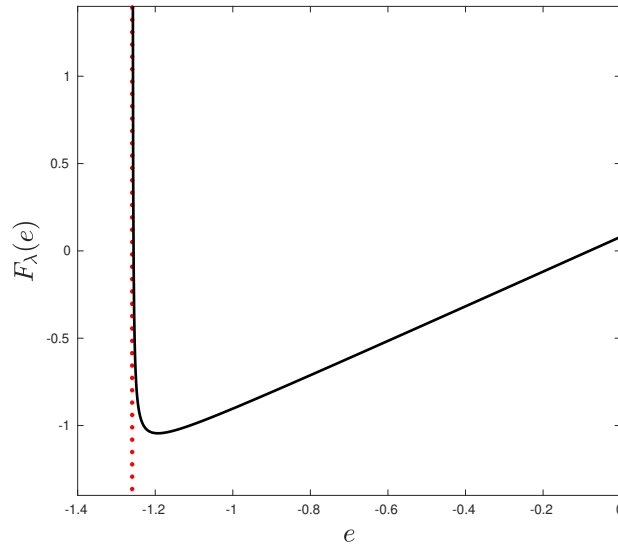


Figure 1: The function $F_\lambda(e)$.

Lemma 3.8. *For $\lambda > 0$, the function $F_\lambda(e)$ is strictly convex on I_λ ; that is, $(\partial_{ee}^2 F)(\lambda, e) > 0$.*

Proof. We have:

$$(\partial_e F)(\lambda, e) = 1 + G'(e(\lambda)) \sum_{i=1}^p \left(\frac{a_i}{a_i G(e(\lambda)) - \lambda} \right)^2 \omega_i \quad (45)$$

and

$$(\partial_{ee}^2 F)(\lambda, e) = G''(e) \sum_{i=1}^p \left(\frac{a_i}{a_i G(e) - \lambda} \right)^2 \omega_i - 2G'(e)^2 \sum_{i=1}^p \left(\frac{a_i}{a_i G(e) - \lambda} \right)^3 \omega_i. \quad (46)$$

Now whenever $e \in I_\lambda$, we have $e > -1/\gamma b^* \geq -1/\gamma b_j$ for all $1 \leq j \leq n$, and $G(e) < \lambda/a^* \leq \lambda/a_i$ for all $1 \leq i \leq p$; consequently,

$$G''(e) = 2\gamma^2 \sum_{j=1}^n \left(\frac{b_j}{1 + \gamma b_j e} \right)^3 \pi_j > 0 \quad (47)$$

and

$$\sum_{i=1}^p \left(\frac{a_i}{a_i G(e) - \lambda} \right)^3 \omega_i < 0. \quad (48)$$

Consequently, $(\partial_{ee}^2 F)(\lambda, e) > 0$ for all $e \in I_\lambda$, i.e. the function $F_\lambda(e)$ is convex. \square

Lemma 3.9. *The function $F_\lambda(e)$ diverges to $+\infty$ as $e \rightarrow +\infty$ and as e approaches the left endpoint of I_λ from the right*
Proof. This is immediate from the definition of $F(\lambda, e)$. \square

Lemma 3.10. *For each $\lambda > \lambda^*$, $F(\lambda, 0) > 0$.*

Proof. We have:

$$F(\lambda, 0) = - \sum_{i=1}^p \frac{a_i \omega_i}{a_i G(0) - \lambda}. \quad (49)$$

Since $G(e(\lambda)) < \lambda/a_i$ and $G(e)$ is decreasing on I_λ , and $e(\lambda) < 0$, we also have $G(0) < G(e(\lambda)) < \lambda/a_i$; consequently, $F(\lambda, 0) > 0$. \square

Proposition 3.11. *For $\lambda > \lambda^*$, $(\partial_e F)(\lambda, e(\lambda)) > 0$.*

Proof. This follows from (43) and $e'(\lambda) > 0$. \square

We have shown that $F_\lambda(e)$ has two roots in the interval $I_\lambda \cap (-\infty, 0)$ whenever $\lambda > \lambda^*$. Proposition 3.11 identifies $e(\lambda)$ as the root that is closest to zero, or equivalently, the root where the derivative of F_λ is positive. This characterization will be used in Section 4.2 to devise the algorithm for computing $e(\lambda)$, and consequently $s(\lambda)$.

3.3 The minimum of $F_\lambda(e)$

We will let $t(\lambda)$ denote the minimum of $F_\lambda(e)$ on J_λ ; that is, $t(\lambda)$ is the unique value on J_λ that satisfies

$$(\partial_e F)(\lambda, t(\lambda)) = 0. \quad (50)$$

We define the function $Q(\lambda)$ for $\lambda > 0$ by:

$$Q(\lambda) = F(\lambda, t(\lambda)). \quad (51)$$

For any $\lambda > 0$, we define the function $R_\lambda(e)$ for $e \in I_\lambda$ by:

$$R_\lambda(e) = (\partial_e F)(\lambda, e) = F'_\lambda(e). \quad (52)$$

Note that by definition, $R_\lambda(t(\lambda)) = 0$ for all $\lambda > 0$.

We will show that Q is decreasing and convex and R_λ is increasing and concave.

Lemma 3.12. *$Q(\lambda)$ is a decreasing function of $\lambda > 0$.*

Proof. The derivative of Q may be computed as follows:

$$\begin{aligned} Q'(\lambda) &= \partial_\lambda \{F(\lambda, t(\lambda))\} \\ &= (\partial_\lambda F)(\lambda, t(\lambda)) + (\partial_e F)(\lambda, t(\lambda)) t'(\lambda) \\ &= (\partial_\lambda F)(\lambda, t(\lambda)) \\ &= - \sum_{i=1}^p \frac{a_i \omega_i}{(a_i G(t(\lambda)) - \lambda)^2}, \end{aligned} \quad (53)$$

which is negative. \square

Proposition 3.13. *$Q(\lambda)$ is a convex function of $\lambda > 0$.*

Proof. We first compute the derivative of $t(\lambda)$. We have

$$0 = (\partial_e F)(\lambda, t(\lambda)). \quad (54)$$

Differentiating with respect to λ , we find

$$0 = (\partial_{\lambda e}^2 F)(\lambda, t(\lambda)) + (\partial_{ee}^2 F)(\lambda, t(\lambda))t'(\lambda), \quad (55)$$

and so

$$\begin{aligned} t'(\lambda) &= \frac{-(\partial_{\lambda e}^2 F)(\lambda, t(\lambda))}{(\partial_{ee}^2 F)(\lambda, t(\lambda))} \\ &= \frac{-2G'(t(\lambda)) \sum_{i=1}^p \frac{a_i^2 \omega_i}{(a_i G(t(\lambda)) - \lambda)^3}}{G''(t(\lambda)) \sum_{i=1}^p \frac{a_i^2 \omega_i}{(a_i G(t(\lambda)) - \lambda)^2} - 2G'(e)^2 \sum_{i=1}^p \frac{a_i^3 \omega_i}{(a_i G(t(\lambda)) - \lambda)^3}}. \end{aligned} \quad (56)$$

Now the second derivative of Q is given by

$$Q''(\lambda) = 2 \sum_{i=1}^p \frac{a_i(a_i G'(t(\lambda))t'(\lambda) - 1)\omega_i}{(a_i G(t(\lambda)) - \lambda)^3}. \quad (57)$$

We will show that $Q''(\lambda) > 0$ for all λ . In fact, we will show the stronger result that each summand is positive, or equivalently, recalling that $a^* = \max_{1 \leq i \leq p} a_i$,

$$a^* G'(t(\lambda))t'(\lambda) \leq 1. \quad (58)$$

To prove this, we observe that

$$\begin{aligned} a^* G'(t(\lambda))t'(\lambda) &= \frac{-2G'(t(\lambda))^2 \sum_{i=1}^p \frac{a_i^3 \omega_i}{(a_i G(t(\lambda)) - \lambda)^3} \frac{a^*}{a_i}}{G''(t(\lambda)) \sum_{i=1}^p \frac{a_i^2 \omega_i}{(a_i G(t(\lambda)) - \lambda)^2} - 2G'(t(\lambda))^2 \sum_{i=1}^p \frac{a_i^3 \omega_i}{(a_i G(t(\lambda)) - \lambda)^3}} \\ &= \frac{-2G'(t(\lambda))^2 \sum_{i=1}^p \frac{a_i^3 \omega_i}{(a_i G(t(\lambda)) - \lambda)^3} \frac{a^*}{a_i}}{G''(t(\lambda)) \sum_{i=1}^p \frac{a_i^3 \omega_i}{(a_i G(t(\lambda)) - \lambda)^3} \frac{a_i G(t(\lambda)) - \lambda}{a_i} - 2G'(t(\lambda))^2 \sum_{i=1}^p \frac{a_i^3 \omega_i}{(a_i G(t(\lambda)) - \lambda)^3}} \\ &= \frac{-2G'(t(\lambda))^2 \sum_{i=1}^p \frac{a_i^3 \omega_i}{(a_i G(t(\lambda)) - \lambda)^3} \frac{a^*}{a_i}}{\sum_{i=1}^p \frac{a_i^3 \omega_i}{(a_i G(t(\lambda)) - \lambda)^3} \left(G''(t(\lambda)) \frac{a_i G(t(\lambda)) - \lambda}{a_i} - 2G'(t(\lambda))^2 \right)} \\ &= \frac{\sum_{i=1}^p \frac{a_i^3 \omega_i}{(\lambda - a_i G(t(\lambda)))^3} \frac{a^*}{a_i}}{\sum_{i=1}^p \frac{a_i^3 \omega_i}{(\lambda - a_i G(t(\lambda)))^3} \left(1 - \frac{G''(t(\lambda))}{2G'(t(\lambda))^2} \frac{a_i G(t(\lambda)) - \lambda}{a_i} \right)}. \end{aligned} \quad (59)$$

To show that this is less than 1, it is enough to show that

$$\frac{a^*}{a_i} \leq 1 - \frac{G''(t(\lambda))}{2G'(t(\lambda))^2} \frac{a_i G(t(\lambda)) - \lambda}{a_i} = 1 - \frac{G''(t(\lambda))}{2G'(t(\lambda))^2} \left(G(t(\lambda)) - \frac{\lambda}{a_i} \right), \quad (60)$$

or equivalently

$$1 \leq \frac{a_i}{a^*} + \frac{G''(t(\lambda))}{2G'(t(\lambda))^2} \left(\frac{\lambda}{a^*} - \frac{a_i}{a^*} G(t(\lambda)) \right), \quad (61)$$

We will show that this inequality holds for any value of a_i between 0 and a^* . If $a_i = a^*$, then the right side becomes

$$1 + \frac{G''(t(\lambda))}{2G'(t(\lambda))^2} \left(\frac{\lambda}{a^*} - G(t(\lambda)) \right), \quad (62)$$

and since the term

$$\frac{G''(t(\lambda))}{2G'(t(\lambda))^2} \left(\frac{\lambda}{a^*} - G(t(\lambda)) \right) \quad (63)$$

is positive (because G is convex, $t(\lambda) \in J_\lambda$, and $a^* G(e) < \lambda$ on J_λ), the desired inequality is satisfied.

On the other hand, if $a_i = 0$, the right hand side becomes

$$\frac{G''(t(\lambda))}{2G'(t(\lambda))^2} \frac{\lambda}{a^*} > \frac{G''(t(\lambda))G(\lambda)}{2G'(t(\lambda))^2} \quad (64)$$

where the inequality holds since $t(\lambda) \in J_\lambda$, and $a^*G(e) < \lambda$ for all $e \in J_\lambda$. By the Cauchy-Schwarz inequality,

$$\begin{aligned}
|G'(\lambda)| &= \gamma \sum_{j=1}^n \left(\frac{b_j}{1 + \gamma b_j e} \right)^2 \pi_j = \gamma \sum_{j=1}^n \left(\frac{b_j}{1 + \gamma b_j e} \right)^{3/2} \left(\frac{b_j}{1 + \gamma b_j e} \right)^{1/2} \pi_j \\
&\leq \left[\gamma^2 \sum_{j=1}^n \left(\frac{b_j}{1 + \gamma b_j e} \right)^3 \pi_j \right]^{1/2} \left[\sum_{j=1}^n \frac{b_j}{1 + \gamma b_j e} \pi_j \right]^{1/2} \\
&= \sqrt{\frac{G''(e)G(e)}{2}},
\end{aligned} \tag{65}$$

or in other words,

$$\frac{G''(e)G(e)}{2G'(e)^2} \geq 1. \tag{66}$$

This gives the desired result. \square

Proposition 3.14. *For all $\lambda > 0$, $R_\lambda(e)$ is an increasing and concave function of $e \in I_\lambda$.*

Proof. The first derivative of R_λ is:

$$R'_\lambda(e) = (\partial_{ee}^2 F)(\lambda, e), \tag{67}$$

which as we've seen is positive. The second derivative of R_λ is

$$\begin{aligned}
R''_\lambda(e) &= (\partial_{eee}^3 F)(\lambda, e) \\
&= G^{(3)}(e) \sum_{i=1}^p \left(\frac{a_i}{a_i G(e) - \lambda} \right)^2 \omega_i - 6G''(e)G'(e) \sum_{i=1}^p \left(\frac{a_i}{a_i G(e) - \lambda} \right)^3 \omega_i \\
&\quad + 6G'(e)^3 \sum_{i=1}^p \left(\frac{a_i}{a_i G(e) - \lambda} \right)^4 \omega_i,
\end{aligned} \tag{68}$$

which is always negative, since $G^{(3)}(e) < 0$, $G''(e) > 0$, $G'(e) < 0$, and $a_i G(e) < \lambda$ for all $e \in I_\lambda$ and $1 \leq i \leq p$. \square

4 Algorithms

In this section, we describe the algorithms for computing the boundary λ^* and for evaluating the Stieltjes transform $s(\lambda)$ and its derivative $s'(\lambda)$.

4.1 Computation of the boundary λ^*

In this section, we derive an algorithm for the computation of λ^* . First, we observe that when $\lambda > \lambda^*$, then as we have shown there are real roots of $F_\lambda(e)$ to the left and to the right of $t(\lambda)$; in particular, $F(\lambda, t(\lambda)) < 0$. On the other hand, if $\lambda < \lambda^*$, the function $F_\lambda(e)$ cannot have a real root, since that would imply that the Stieltjes transform is real inside the support of μ . Consequently, $F(\lambda, t(\lambda)) > 0$. It follows that the bulk edge λ^* is the value at which $F(\lambda, t(\lambda)) = 0$; that is, λ^* , is the unique root of Q on $(0, \infty)$.

From Lemma 3.12 and Proposition 3.13, $Q(\lambda)$ is decreasing and convex. With an efficient procedure for evaluating $Q(\lambda)$ and $Q'(\lambda)$, we can therefore use Newton's algorithm to find its root if we initialize the algorithm to the left of the root. In Section 4.1.2, we detail how to evaluate $Q(\lambda)$ and $Q'(\lambda)$. As a preliminary step, we will need to compute the left endpoint of I_λ ; we do this in 4.1.1. The resulting algorithm for evaluating λ^* is summarized in Algorithm 3.

Algorithm 1 Computation of the left endpoint of I_λ

- 1: **Input:** Precision $\epsilon > 0$; parameter $\lambda > 0$
 - 2: **Initialize:** $e > -1/(\gamma b^*)$
 - 3: **Bisection:** $e \leftarrow (e - 1/(\gamma b^*))/2$, until $T_\lambda(e) > 0$
 - 4: **Newton:** $e \leftarrow e - T_\lambda(e)/T'_\lambda(e)$, until $|T_\lambda(e)| < \epsilon$
 - 5: **Output:** $e_\lambda^* = e$
-

Algorithm 2 Evaluation of $t(\lambda)$, $Q(\lambda)$ and $Q'(\lambda)$

- 1: **Input:** Precision $\epsilon > 0$; parameter $\lambda > 0$
 - 2: **Endpoint:** Compute e_λ^* using Algorithm 1
 - 3: **Initialize:** $e > e_\lambda^*$
 - 4: **Bisection:** $e \leftarrow (e + e_\lambda^*)/2$, until $R_\lambda(e) < 0$
 - 5: **Newton:** $e \leftarrow e - R_\lambda(e)/R'_\lambda(e)$, until $|R_\lambda(e)| < \epsilon$
 - 6: **Output:** $t(\lambda) = e$, $Q(\lambda) = F(\lambda, e)$, $Q'(\lambda) = (\partial_\lambda F)(\lambda, e)$
-

Algorithm 3 Evaluation of λ^*

- 1: **Input:** Precision $\epsilon > 0$
 - 2: **Initialize:** $\lambda > 0$
 - 3: **Bisection:** $\lambda \leftarrow \lambda/2$, until $Q(\lambda) < 0$
 - 4: **Newton:** $\lambda \leftarrow \lambda - Q(\lambda)/Q'(\lambda)$, until $|Q(\lambda)| < \epsilon$
 - 5: **Output:** $\lambda^* = \lambda$
-

4.1.1 Computation of the left endpoint of I_λ , $\lambda > 0$

We recall the definition of the interval I_λ :

$$I_\lambda = \left\{ e \in J : G(e) < \frac{\lambda}{a^*} \right\}, \quad (69)$$

where J is the interval $J = \{e : e > -1/(\gamma b^*)\}$. Let us denote by e_λ^* the left endpoint of I_λ . Since $G(e)$ is a decreasing function of e on J , e_λ^* is the unique root of

$$T_\lambda(e) = G(e) - \frac{\lambda}{a^*} \quad (70)$$

on J . Since T_λ is a decreasing, convex function of e on J , we may find its root using Newton's algorithm, initialized to the left of the root. Such an initial value e_0 can be found by starting with any value e in J , and performing bisection with $-1/(\gamma b^*)$, the left endpoint of J , until we arrive at a value where $T_\lambda(e_0) > 0$. Newton's algorithm is then performed with initial value e_0 . We summarize the procedure in Algorithm 1.

4.1.2 Evaluation of $t(\lambda)$, $Q(\lambda)$, and $Q'(\lambda)$

Next, we show how to evaluate the functions $t(\lambda)$, $Q(\lambda)$, and $Q'(\lambda)$. $t(\lambda)$ is defined as the root of $R_\lambda(e)$ on I_λ . Since $R_\lambda(e)$ is an increasing, concave function, we may find its root using the Newton algorithm initialized to the left of the root, i.e. the region where $R_\lambda(e) < 0$. Such an initial value may be found by taking a starting point e to the right of e_λ^* , and performing bisection on e and e_λ^* until we arrive at a value e_0 with $R_\lambda(e_0) < 0$. We can then perform Newton's algorithm on R_λ , initialized at e_0 . The procedure is summarized in Algorithm 2.

4.2 Evaluation of $s(\lambda)$ and $s'(\lambda)$, $\lambda > \lambda^*$

In this section, we present an algorithm for evaluating the Stieltjes transform $s(\lambda)$ of μ , and its derivative $s'(\lambda)$, when $\lambda > \lambda^*$. This immediately provides a method for evaluating $\underline{s}(\lambda)$ and $\underline{s}'(\lambda)$, and the D -transform $D(\lambda)$ defined in Section 2.3.

As we showed in Section 3.2, the function $F_\lambda(e)$ is convex on I_λ and has two roots, both of which are negative. The root closest to 0, i.e. the rightmost root, is $e(\lambda)$. Since $F_\lambda(0) > 0$ and $F_\lambda(e)$ is convex, this tells us that Newton's method, initialized at $e_0 = 0$, will converge to $e(\lambda)$. For brevity, we introduce the function $W(\lambda, e)$ defined by:

$$W(\lambda, e) = \sum_{i=1}^p \frac{\omega_i}{a_i G(e) - \lambda}. \quad (71)$$

With this notation, we have:

$$s(\lambda) = W(\lambda, e(\lambda)) \quad (72)$$

and

$$s'(\lambda) = (\partial_\lambda W)(\lambda, e(\lambda)) + (\partial_e W)(\lambda, e(\lambda))e'(\lambda). \quad (73)$$

Note that from (42), we can evaluate $e'(\lambda)$:

$$e'(\lambda) = \frac{-(\partial_\lambda F)(\lambda, e(\lambda))}{(\partial_e F)(\lambda, e(\lambda))}. \quad (74)$$

The method for evaluating $s(\lambda)$ and $s'(\lambda)$ is summarized in Algorithm 4.

Algorithm 4 Evaluation of $s(\lambda)$ and $s'(\lambda)$

- 1: **Input:** Precision $\epsilon > 0$; parameter $\lambda > \lambda^*$
 - 2: **Initialize:** $e = 0$
 - 3: **Newton:** $e \leftarrow e - F_\lambda(e)/F'_\lambda(e)$, until $|F_\lambda(e)| < \epsilon$
 - 4: **Output:** $s(\lambda) = W(\lambda, e)$, $s'(\lambda) = (\partial_\lambda W)(\lambda, e) - (\partial_e W)(\lambda, e)(\partial_\lambda F)(\lambda, e)/(\partial_e F)(\lambda, e)$
-

5 Numerical results

We have implemented the algorithms described in Section 4 in MATLAB 2017b. The numerical experiments we report here were carried out on a Dell XPS 13 laptop with 15.6 Gb of RAM and an Intel Core i7-3632QM CPU running at 2.20GHz. The code will be made available online at the author’s Github page at a future date.

5.1 Convergence

Algorithms 1 – 4 are all versions of the Newton root-finding method. In this section, we illustrate the quadratic convergence of these methods, as predicted from the theory reviewed in Section 2.4. In each experiment, we used parameters $p = 512$, $n = 1024$, and $\gamma = 1/2$. We generated the values a_1, \dots, a_p and b_1, \dots, b_n randomly from a $\text{Unif}(0, 1)$ distribution, and assigned random probabilities ω_i and π_j by drawing values from $\text{Unif}(0, 1)$ and normalizing to sum to 1. For experiments in which a value λ is specified, we also choose it at random.

In Tables 1 – 4, the first column displays the iteration number m , starting from the initial value and going until the root has been reached. The second column displays the function value at the m^{th} iterate; the algorithm terminates when the function reaches machine precision ϵ . We work in double precision, so $\epsilon \approx 10^{-16}$. The third column displays the relative error in the root itself, defined by:

$$\text{err}(x_m, x) = \frac{x_m - x}{x}. \quad (75)$$

Table 1 shows the results for Algorithm 1, which computes the left endpoint e_λ^* of I_λ . Table 2 shows the results for Algorithm 2, which evaluates $t(\lambda)$. Table 3 shows the results for Algorithm 3, which computes the boundary λ^* . Table 4 shows the results for Algorithm 4, which evaluates $e(\lambda)$. For each algorithm, we observe quadratic convergence close to the root, as expected. That is, on each iteration close to termination the number of correct digits roughly doubles, and the size of the objective roughly squares, until machine precision is reached.

5.2 Scalability

In the next experiment, we compute timings for the computation of λ^* and the evaluation of $s(\lambda)$. In detail, we fix the parameter $\gamma = 1/2$. For increasing values of n , we set $p = n/2$. We draw a_1, \dots, a_p and b_1, \dots, b_n independently from a $\text{Unif}(0, 1)$ distribution. We generated the values a_1, \dots, a_p and b_1, \dots, b_n randomly from a $\text{Unif}(0, 1)$ distribution, and assigned them random probabilities ω_i and π_j by drawing values from $\text{Unif}(0, 1)$ and normalizing to sum to 1.

For each n , we then record the CPU time required to compute λ^* , and the CPU time required to compute $s(\lambda)$ on a grid of 100 equispaced values of λ . The reported timings are averaged over five runs of the experiment, and are displayed in Table 5. It is apparent that the running times scale linearly with n , as we would expect.

In addition to linearly scaling with n , the magnitudes of the timings are quite encouraging; for example, it takes less than 12 seconds to compute λ^* when n is over two million and p is over one million. We note too that we have made only minimal efforts to optimize the code in its current implementation; for example, we have not made any attempts to determine a good initialization for Newton’s method.

Acknowledgements

This work was supported by the NSF BIGDATA program, IIS 1837992. I thank Edgar Dobriban for a helpful discussion and for pointing out the method from [11].

References

- [1] Zhidong Bai and Jack W. Silverstein. *Spectral Analysis of Large Dimensional Random Matrices*. Springer Series in Statistics. Springer, 2009.
- [2] Florent Benaych-Georges and Raj Rao Nadakuditi. The singular values and vectors of low rank perturbations of large rectangular random matrices. *Journal of Multivariate Analysis*, 111:120–135, 2012.
- [3] Andreas Buja and Nermin Eyuboglu. Remarks on parallel analysis. *Multivariate Behavioral Research*, 27(4):509–540, 1992.
- [4] Lucilio Cordero-Grande. Numerical techniques for the computation of sample spectral distributions of population mixtures. *arXiv preprint arXiv:1812.05575*, 2018.

- [5] Romain Couillet and Merouane Debbah. *Random Matrix Methods for Wireless Communications*. Cambridge University Press, 2011.
- [6] Romain Couillet and Walid Hachem. Analysis of the limiting spectral measure of large random matrices of the separable covariance type. *Random Matrices: Theory and Applications*, 3(4), 2014.
- [7] Germund Dahlquist and Åke Björck. *Numerical Methods*. Prentice Hall, Inc., 1974.
- [8] Edgar Dobriban. Efficient computation of limit spectra of sample covariance matrices. *Random Matrices: Theory and Applications*, 4(4), 2015.
- [9] Edgar Dobriban. Permutation methods for factor analysis and PCA. *arXiv preprint arXiv:1710.00479*, 2017.
- [10] Edgar Dobriban, William Leeb, and Amit Singer. Optimal prediction in the linearly transformed spiked model. *arXiv preprint arXiv:1709.03393*, 2017.
- [11] Edgar Dobriban and Art B. Owen. Deterministic parallel analysis: an improved method for selecting factors and principal components. *Journal of the Royal Statistical Society: Series B (Statistical Methodology)*, 2018.
- [12] David L. Donoho, Matan Gavish, and Iain M Johnstone. Optimal shrinkage of eigenvalues in the spiked covariance model. *Annals of Statistics*, 46(6), 2018.
- [13] Matan Gavish and David L. Donoho. Optimal shrinkage of singular values. *IEEE Transactions on Information Theory*, 63(4):2137–2152, 2017.
- [14] Walid Hachem, Philippe Loubaton, and Jamal Najim. Deterministic equivalents for certain functionals of large random matrices. *The Annals of Applied Probability*, 17(3):875–930, 2007.
- [15] Walid Hachem, Philippe Loubaton, and Jamal Najim. A CLT for information-theoretic statistics of gram random matrices with a given variance profile. *The Annals of Applied Probability*, 18(6):2071–2130, 2008.
- [16] David Hong, Laura Balzano, and Jeffrey A. Fessler. Towards a theoretical analysis of PCA for heteroscedastic data. In *54th Annual Allerton Conference on Communication, Control, and Computing*, pages 496–503. IEEE, 2016.
- [17] David Hong, Laura Balzano, and Jeffrey A. Fessler. Asymptotic performance of PCA for high-dimensional heteroscedastic data. *Journal of Multivariate Analysis*, 2018.
- [18] David Hong, Laura Balzano, and Jeffrey A. Fessler. Optimally Weighted PCA for High-Dimensional Heteroscedastic Data. *arXiv preprint arXiv:1810.12862*, 2018.
- [19] John L. Horn. A rationale and test for the number of factors in factor analysis. *Psychometrika*, 30(2):179–185, 1965.
- [20] Shira Kritchman and Boaz Nadler. Determining the number of components in a factor model from limited noisy data. *Chemometrics and Intelligent Laboratory Systems*, 94(1):19–32, 2008.
- [21] Shira Kritchman and Boaz Nadler. Non-parametric detection of the number of signals: Hypothesis testing and random matrix theory. *IEEE Transactions on Signal Processing*, 57(10):3930–3941, 2009.
- [22] Olivier Ledoit and Michael Wolf. Spectrum estimation: A unified framework for covariance matrix estimation and PCA in large dimensions. *Journal of Multivariate Analysis*, 139:360–384, 2015.
- [23] Olivier Ledoit and Michael Wolf. Numerical implementation of the QuEST function. *Computational Statistics & Data Analysis*, 115:199–223, 2017.
- [24] William Leeb. Matrix denoising for weighted loss functions and heterogeneous signals. *arXiv preprint arXiv:1902.09474*, 2019.
- [25] William Leeb and Elad Romanov. Optimal spectral denoising and PCA with heteroskedastic noise. *arXiv preprint arXiv:1811.02201v2*, 2019.
- [26] Vladimir A Marchenko and Leonid A Pastur. Distribution of eigenvalues for some sets of random matrices. *Mat. Sb.*, 114(4):507–536, 1967.
- [27] Raj Rao Nadakuditi. Optshrink: An algorithm for improved low-rank signal matrix denoising by optimal, data-driven singular value shrinkage. *IEEE Transactions on Information Theory*, 60(5):3002–3018, 2014.
- [28] Yurii Nesterov. *Lectures on Convex Optimization*, volume 137 of *Springer Optimization and Its Applications*. Springer, 2nd edition, 2018.
- [29] Damien Passemier and Jian-Feng Yao. On determining the number of spikes in a high-dimensional spiked population model. *Random Matrices: Theory and Applications*, 1(01):1150002, 2012.
- [30] Debashis Paul. Asymptotics of sample eigenstructure for a large dimensional spiked covariance model. *Statistica Sinica*, 17(4):1617–1642, 2007.
- [31] Debashis Paul and Jack W. Silverstein. No eigenvalues outside the support of the limiting empirical spectral distribution of a separable covariance matrix. *Journal of Multivariate Analysis*, 100:37–57, 2009.
- [32] Jack W. Silverstein. Strong convergence of the empirical distribution of eigenvalues of large dimensional random matrices. *Journal of Multivariate Analysis*, 55:331–339, 1995.
- [33] Jack W. Silverstein and Z.D. Bai. On the empirical distribution of eigenvalues of a class of large dimensional random matrices. *Journal of Multivariate Analysis*, 54:175–192, 1995.
- [34] Terence Tao. *Topics in random matrix theory*, volume 132. American Mathematical Society, 2012.
- [35] Anru Zhang, T. Tony Cai, and Yihong Wu. Heteroskedastic PCA: Algorithm, optimality, and applications. *arXiv preprint arXiv:1810.08316*, 2018.

Table 1: Error after each iterate in evaluation of e_λ^* .

m	$T_\lambda(e_m)$	$\text{err}(e_m, e_\lambda^*)$
1	2.08e-01	4.26e-02
2	4.34e-02	1.11e-02
3	2.55e-03	6.90e-04
4	9.66e-06	2.63e-06
5	1.40e-10	3.80e-11
6	-2.75e-16	-1.23e-16

Table 2: Error after each iterate in evaluation of $t(\lambda)$.

m	$R_\lambda(e_m)$	$\text{err}(e_m, t(\lambda))$
1	-3.77e-01	3.71e-02
2	-6.89e-02	8.34e-03
3	-3.40e-03	4.34e-04
4	-9.24e-06	1.18e-06
5	-6.84e-11	8.73e-12
6	-5.55e-15	7.85e-16

Table 3: Error after each iterate in evaluation of λ^* .

m	$Q(\lambda_m)$	$\text{err}(\lambda_m, \lambda^*)$
1	1.25e+00	-3.10e-01
2	3.10e-01	-1.03e-01
3	3.12e-02	-1.15e-02
4	3.92e-04	-1.46e-04
5	6.34e-08	-2.37e-08
6	2.00e-15	-2.11e-16

Table 4: Error after each iterate in evaluation of $e(\lambda)$.

m	$F_\lambda(e_m)$	$\text{err}(e_m, e(\lambda))$
1	4.71e-01	-1.00e+00
2	8.86e-03	-1.93e-02
3	6.42e-06	-1.40e-05
4	3.43e-12	-7.50e-12
5	4.44e-16	-1.10e-15

Table 5: Timings in seconds for evaluating λ^* and $s(\lambda)$ at 100 values of λ

$\log_2(n)$	Timing, λ_*	Timing, $s(\lambda)$
12	3.41e-02	3.33e-02
13	5.35e-02	4.39e-02
14	1.00e-01	7.55e-02
15	1.93e-01	1.38e-01
16	3.85e-01	2.60e-01
17	6.98e-01	4.13e-01
18	1.35e+00	7.79e-01
19	2.83e+00	1.87e+00
20	5.86e+00	4.24e+00
21	1.15e+01	8.70e+00